Observation of Solidification of Oils under High Pressure

Conference Paper · January 1985

CITATIONS
3

READS
11

3 authors, including:

Nobuyoshi Ohno
Saga University
140 PUBLICATIONS **595** CITATIONS

SEE PROFILE

PROCEEDINGS OF THE J S L E INTERNATIONAL TRIBOLOGY CONFERENCE
July 8-10, 1985, Tokyo, Japan

Observation of Solidification of Oils under High Pressure

Fujio HIRANO* Noriyuku KUWANO** Nobuyoshi OHNO**

In view of the significant effect of the glass transition of oils on performances of machine elements in rolling contact direct observation on their solidification processes was carried out utilizing a high pressure viscometer furnished with sapphire windows.

First, in order to verify the possibility of the observation by applying this method, the chain-matching effect of hydrocarbons with fatty acid additives was investigated. Their freezing pressures were easily determined by appearances of crystallines quite similar to those observed under atmospheric pressure and showed minima under the matching condition.

On the other hand, the glass transition of mineral oils was characterized by dense crowds of atomized particles. Blended oils with wide-ranged molecular weight distributions exhibited transition points lower than those of base oils with narrow-ranged ones.

Results of impact tests showed also appearances of crystallines or atomized particles in high pressure ranges under the Hertzian condition where hydrocarbons or oils were entrapped.

1. INTRODUCTION

Behaviours of lubricating oils under high pressures such as in elastohydrodynamic contacts are not only of academic interest but also of practical importance in relation to performances of traction transmission. Under these conditions contact pressures often exceed 1~2 GPa, where, oils exhibit solid-like behaviours (1). These phenomena are generally denoted by the glass transition or viscoelastic transition. Solidified oils show the same type of properties as ductile metals characterized by the existence of the shear trength.

Concerning models of lubricants under high pressures Gentle and Paul (2) and Alsaad, Bair, Sanborn and Winer (3) discussed the characteristic properties of the glass transition in connection with methods of observation and influences of environmental conditions, e. g. isobaric cooling or isothermal compression.

On the other hand, Gentle and Cameron (4) estimated the pour-points of oils under the elastohydrodynamic contact condition each other. They suggested also the possibility to treat shear behaviours of oils under high pressure as those of granular beds (5).

Concerning elastohydrodynamic behaviours of oil films between elastic bodies normally approaching, a number of experimental investigations show evidence of entrapment of lubricant in Hertzian contact (6,7).

The glass transition phenomena of the entrapped lubricants were also discussed in the reference (3) and (4). However, there are few experimental investigations directly observing the solidification phenomena. The present paper deals with the visual observation of the glassy state in bulk and in Hertzian contacts as well as the estimation of the glass transition pressure or temperature in bulk.

2. EXPERIMENTALS

2.1 Experimental Conditions

The experimental series in the present investigation were chosen combining three categories of conditions:

A. Static condition by isothermal compression,
B. Dynamic condition, i.e. entrapment in Hertzian contacts,
C. Squeeze out of entrapped lubricant;

and

1. crystallization or phase transition of

* Oita Technical College,
1666, Maki, Oita-shi, Oita, Japan
** Saga University,
1, Honjo-machi, Saga-shi, Saga, Japan

normal paraffins containing fatty acids,
2. glass transition of mineral oils.

The series 1 were carried out particularly in relation to the chain-matching phenomena (8). On the other hand, the series 2 aimed to investigate the effect of the molecular weight distribution of mineral oils on lubrication performances of actual machine elements (9-11).

The physical and chemical properties of these lubricants are listed in Table 1-4.

2.2 Experimental apparatuses and procedures

a) Apparatuses for A --- viscometry, A-a

A high pressure viscometer of the falling ball type designed by Saga university was utilized. As shown in Fig. 1 oil is pressurized in a cylindrical space, 12 mm in diameter, by mean of a plunger with a diametral clearance 0.03 mm relative to the inner wall. Results of calibration using di-(2-ethyl-hexyl)sebacate showed sufficient coincidence with the ASME pressure viscosity chart.

The glass transition pressure was determined by estimating a pressure under the isothermal condition showing practically an infinite period to reach the lower terminal.

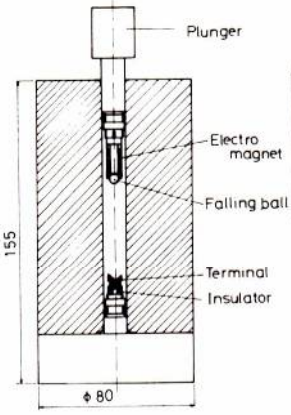

Fig. 1 Viscometer

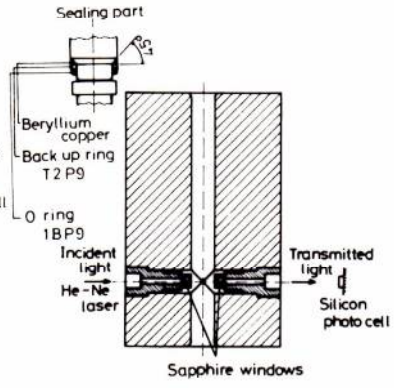

Fig. 2 Direct observation and photometric apparatus

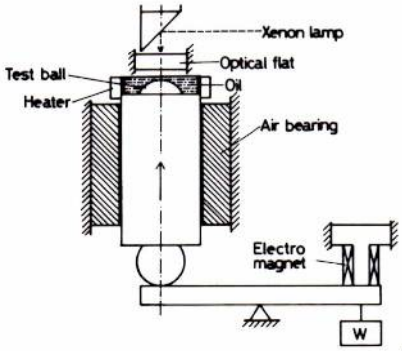

Fig. 3 Interferometer

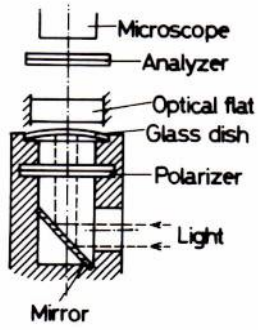

Fig. 4 Direct observation apparatus of entrapment

Table 1. Properties of hydrocarbons

Base liquid	Molecular weight	Specific gravity 20°C	Viscosity mm²/s 37.8°C	Viscosity mm²/s 98.9°C	Melting point °C
n-Octadecane $C_{18}H_{38}$	254.5	0.7765(30°C)	4.38	1.76	28.2
n-Hexadecane $C_{16}H_{34}$	226.45	0.7739	3.04	1.27	18.2
n-Tetradecane $C_{14}H_{30}$	198.39	0.7645	2.08	0.99	5.9
n-Dodecane $C_{12}H_{26}$	170.34	0.7511	1.45	0.73	-9.6

Table 2. Properties of additives

Additive	No.of carbon atoms, n	Name	Molecular weight	Melting point,°C	Specific gravity
Acid $C_{n-1}H_{2n-1}COOH$	4	n-Butyric acid	88.2	-7.9	0.9587(20°C)
	6	n-Caproic acid	116.2	-3.9	0.9240(20°C)
	8	n-Caprylic acid	144.2	16.5	0.9120(20°C)
	10	n-Capric acid	172.3	31.3	0.8858(40°C)
	12	Lauric acid	200.3	43.6	0.8690(50°C)
	14	Myristic acid	228.4	53.8	0.8584(60°C)
	16	Palmitic acid	256.4	62.6	0.8412(80°C)
	18	Stearic acid	284.5	69.3	0.8386(80°C)
	20	Arachic acid	312.5	75.3	0.8240(100°C)

Table 3. Properties of base oils

Oil	Density 15/4 °C	Viscosity, mm²/s 37.8 °C	Viscosity, mm²/s 98.9 °C	$\bar{M}$	Pour Point °C
P60	0.8634	7.8	2.2	264	-10
P150	0.8663	31.4	5.2	398	-17.5
P500	0.8770	106	11.4	533	-12.5
BS	0.8840	464	32.0	741	-12.5
P60′	0.8536	8.3	2.2	270	-12.5
P60D	0.8667	9.1	2.3	274	-40>
P60′D	0.8532	8.8	2.3	275	-40>

Table 4. Properties of blended oils

P60/BS	Viscosity, mm²/s 37.8 °C	Viscosity, mm²/s 98.9 °C	$\bar{M}$
100/0	7.8	2.2	264
80/20	14.6	3.2	303
70/30	21.5	4.4	328
60/40	32.1	5.8	356
50/50	47.7	7.6	390
37/63	80.9	10.7	446
30/70	108	12.9	482
20/80	162	17.2	546
10/90	275	23.6	632
0/100	464	32.0	741

b) Apparatus for A --- dilatometry, A-b

The dilatometric method (3) was also applied in the present experiments. This was quite simply possible with the aid of the same viscometer A-a by observing volumetric changes at prescribed pressures under isothermal conditions. The glass transition is detected by an abrupt change in volume or density.

c) Apparatus for A --- photometry, A-c

In order to detect without delay initiation of the glass formation the cylinder of the viscometer was replaced by another cylinder with sapphire windows enabling photometric or visual observation. As shown in Fig. 2 a decrease in intensity of transmitted light from a He-Ne laser source was detected using silicon photocell.

d) Apparatus A-d and B-d --- interferometry

Fig. 3 shows the apparatus for observing the entrapment of oil between normally approaching elastic bodies. An optical flat of pyrex glass, 15 mm in diameter and 5 mm in thickness of which lower surface is spattered by chromium, is clamped to the upper part. On the other hand, a bearing steel ball, 23.8 mm in diameter, is attached to the upper

end of a spindle supported by an air bearing.

Impact loading is applied to the ball through the spindle by releasing an electromagnet at the end of a lever. The light source for interferometry is a xenon strobscope lamp, which generates monochromatic light with wave length 0.60 μm by passing a red filter. Thus, interference fringes corresponding to the difference of thickner 0.2 μm are obtained. Intensity of impact was varied by changing the dead weight and a gap between the ball and the optical flat.

e) Direct visual observation

The apparatus shown in Fig. 2 is also applicable to direct observation of crystallines or glassy states through the sapphire windows under static condition. Under the Hertzian contact condition, however, it is difficult to discriminate between solidified and liquid states of entrapped lubricant. For this purpose the steel ball was replaced by a transparent dish of pyrex glass, 49 mm in radius of curvature and 2 mm in thickness. This enabled to obtain clear appearances of crystallines with the aid of polarized light as shown Fig.4.

f) Procedure of squeeze out experiments of entrapped lubricants C

In order to observe the transition of entrapped lubricants from solidified to liquid states by interferometric means, the temperature in the contact region after impact with a gap 0.1 mm was raised at a rate of 0.5 K/min.

3. EXPERIMENTAL RESULTS

In the following explanations combinations of the notations of the experimental conditions (A, B and C), lubricants (hydrocarbons 1 and mineral oils 2), and apparatuses (a to e) are used.

Cameron et al. pointed out the presence of the chain-matching effect in boundary lubrication: When numbers of carbon atoms or chain lengths of normal alkane as a solvent and straight chain fatty acid (or alcohol, or amine) as an additive coincide each other, resistance to scuffing becomes highest (12). Afterwards, one of the present authors developed a number of investigations to show further evidences in various aspects relevant to interfacial phenomena (13).

So far the chain-matching effect has been limited within the scope of the interaction between adhesion to solid surfaces and intermolecular cohesion of oriented molecules. In contrast to this aspect of the heterogeneous interaction, the homogeneous interaction between solid and liquid surfaces of the same substance should be considered to clarify the chain-matching effect in essence. In fact, under the matching condition an increase in the freezing temperature under normal pressure from that under non-matching condition was clearly confirmed. Correspondingly, there were also the difference in nucleation of crystallines (15). The present observation dealt with the chain-matching effect on solidification under high pressures.

The properties of the hydrocarbons and fatty acids added to them at a concentration 0.05 mol/l are shown in Table 1 and 2. When the pressure in the cylinder space (A1-b) reached a definite value, the density increased abruptly together with temperature as a result of freezing where abrupt volumetric contraction and generation of heat of solidification occurred. Thus, the freezing pressure were found to be easily determined with accuracy. These freezing pressures are plotted in Fig.5 against the number of carbon atoms of the additives in the base oils n-dodecane (C12), n-tetradecane (C14), and n-hexadecane (C16). It is clearly shown that at each temperature the chain-matching condition brings about the lowest freezing pressures. This corresponds to the lowest freezing temperature in isobaric cooling under the chain-matching conditions (15). The values of n-dodecane in Fig. 5 sufficiently coincide with those reported by Nelson et al. (14).

Fig. 6 shows crystallization at high pressure (A1-e) under the matching and non-matching conditions. Here, the photographs under the matching condition a) C14-acid/C14 and c) C16-acid/C16 exhibit a striking contrast with b) C14-acid/C16 under the non-matching condition.

Under the matching condition numerous minute nuclei appear simultaneously. On the other hand, the non-matching condition is characterized by lengthwise growth of larger fibrous crystallines from small number of

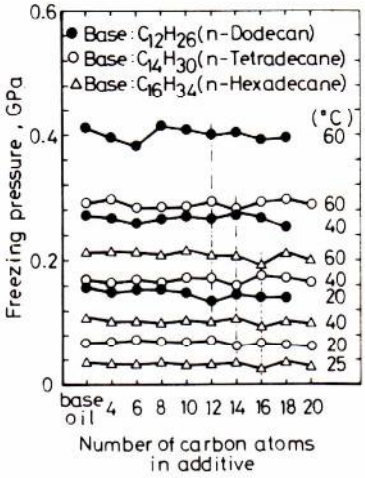

Fig. 5 Freezing pressures

a) C14-acid/C14 b) C14-acid/C16 c) C16-acid/C16

Fig. 6 Direct observation of crystallization at high pressure (40°C) ⌊——⌋ 1 mm

nuclei. These features of the nucleation and the crystal growth were already shown by one of the authors at freezing temperatures under atmospheric pressure, as shown in Fig. 7 (15).

Fig. 8 shows a difference in the entrapment under the impact load with a gap 0.1 mm (B1-d) from that under the static load being increased from 0 to the equal value (A1-d). Under the static load no entrapment was observed as a result of squeeze out of liquid during the increasing load process.

Fig. 9 shows squeeze out of C14-acid/C16 being initially put in a frozen state between the ball and glass surfaces. At elevated temperature the volume of the entrapped lubricant decreases as a result of squeeze out in a liquid state. The melting temperature thus estimated at the Hertzian max. pressure p_H= 0.66 GPa is plotted in Fig. 10, where the peak shows the chain-matching effect.

In view of the fact that the entrapped lubricant exhibits irregular contours in Fig. 9 (B1-d), its solidification is suggested, but the crystalline form is hardly recognized. Fig. 11 shows a direct evidence of the crystallization of C14-acid/C16 in the Hertzian contact (B1-e). Fig. 11 a) is the appearance of 1 min after impact at 17.9°C lower than the freezing temperature under atmospheric pressure. Even when the temperature in the contact region is raised to 30°C higher than the freezing point at atmospheric pressure, the appearance of crystallization still remains unchanged in the central area where the contact pressure is considered to be higher than the freezing pressure, as shown in Fig. 11 b). After cooled again to 18.2°C, recrystallization occurs outside of the contact area in the form of long fibrous crystallines without penetrating in the contact region.

Fig. 12 shows the results of the dilatometric experiments (A2-b) of the base and blended mineral oils listed in Table 3 and 4. In contrast to the series 1 with definite freezing pressures, there is some difficulty in the determination of the transition pressures. The glass transition pressures by the viscometric means (A2-a) are plotted together with the photometric results on the density-pressure curves in Fig. 12 (A2-c).

Fig. 13 shows some example of the direct observation in bulk. Here, it is noted that under high pressures exceeding the glass transition pressures mineral oils at least partly solidify in granular forms. The granular solidification is also observed at temperature lower than pour points at atmospheric pressure. The grain size was estimated as 7 μm on the average in both the cases.

4. DISCUSSIONS

In the series A-1, where the transition

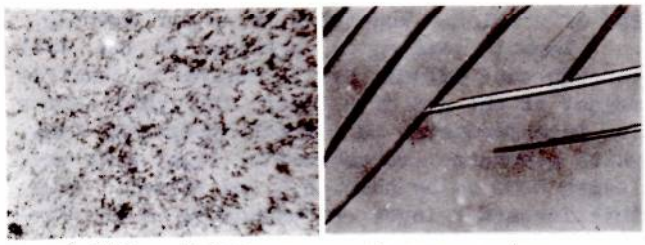

a) C18-acid/C18, 1s b) C6-acid/C16, 10s

Fig. 7 Crystal growth under atmospheric pressure ⟵ 0.1 mm

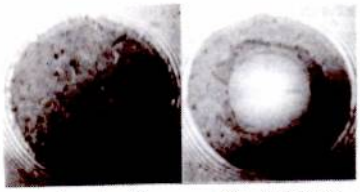

a) static b) impact

Fig. 8 Entrapment of C14-acid/C16 (22°C)

⟵ 0.1 mm

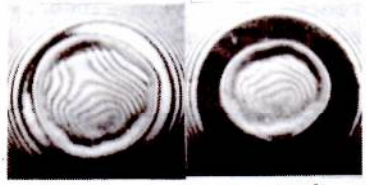

a) 15.6°C b) 50°C

Fig. 9 Squeeze out of C14-acid/C16

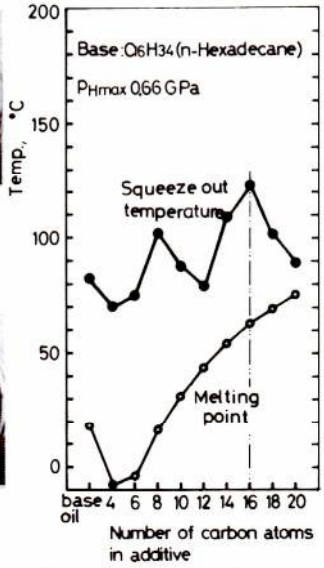

Fig. 10 Squeeze out temperature of solution

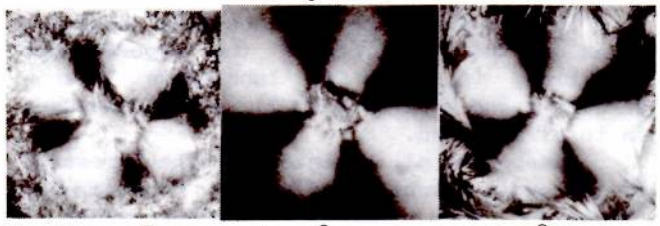

a) 17.9°C b) 30°C c) 18.2°C

Fig. 11 Direct observation in Hertzian contact, C14-acid/C16, p_{Hmax} 0.31 GPa

⟵ 1 mm

occurs quite definitely in the form of the phase change from liquid to solid the dilatometric method A1-b gives accurate freezing pressures. On the other hand, by the viscometric means A1-a some deviation from results of A1-b is recognized. The cause is attributed to an indefinite relation between a position of the falling ball and a domain of initial crystallization.

By the photometric means A1-c, attenuation of intensity of transmitted light begins as soon as initial crystallines are generated on the light path in the cylinder. Thus, some time lag occurs between the initiation of crystallines and freezing as a whole. This

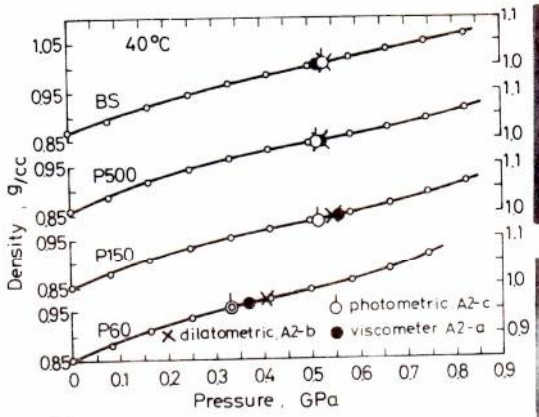

Fig. 12 Density-pressure curves of mineral oils

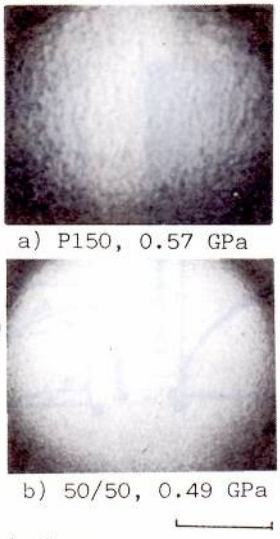

Fig. 13 Direct observation of glassy state of mineral oils, 40°C

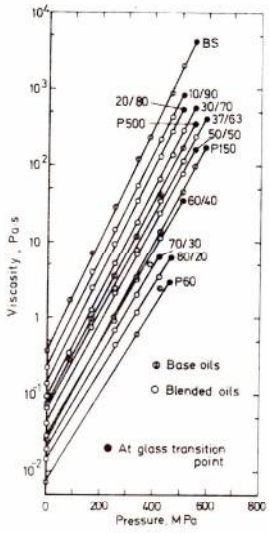

Fig. 14 Viscosity-pressure curves of mineral oils, 42°C

time lag was small in the cases of the hydrocarbons without fatty acid and those under the chain-matching condition. In contrast to these, the non-matching mixtures showed considerable lags, particularly, when numbers of carbon atoms of added fatty acids were large. This fact is considered to be caused by the difference in the crystal structures between initial and eutectis phases.

Next, the situation becomes more complicated in the series A2 of mineral oils containing a variety of components of hydrocarbons in the main, i.e. crystallizable or non-crystallized, with different molecular weight distributions. As shown in Fig. 12, the dilatometric method A2-b is little effective to determine the glass transition pressures. Generally, the viscometric method A2-a exhibits nearly equal values to those estimated from the points of inflexion of the density-pressure curves in Fig. 12. On the other hand, the photometric method A2-c results in lower transition pressures compared with the other methods. This corresponds to initial appearance of solid grains. Consequently, the photometric method is considered to detect the initiation of the glassy state within a definite period. It depends considerably on the observation period.

Considering that wax content in mineral oil has the most predominant influence on its pour point at atmospheric pressure, the effect of dewaxing on the glass transition was additionally investigated. As listed in Table 5, the oil P60D obtained by the dewaxing treatment from P60 results in a considerably higher pressure 0.54 GPa compared with 0.37 GPa of P60. On the other hand, the oil P60´ produced by the hydrofinishing process shows merely a little lower value 0.33 GPa, but the dewaxed oil P60´D an extremely high transition pressure.

Next, as pointed out by one of the authors (9-11), the molecular weight distribution of oils has pronounced influences upon lubricating performances of machine elements, e.g. gears, bearings, seals etc. Fig. 14 shows the glass transition pressures of the base (narrow-ranged) and blended (wide-ranged) oils as terminals of viscosity-pressure curves. It is noted that the base oils, P60, P150, P500, and BS exhibit higher transition pressures compared with the blended oils. Concerning the effect of this difference on the life of ball bearings some discussion was already developed by the authors in connection with the effect of the elastohydrodynamic film formation and oxidation of ball and race surfaces.

Table. 5 Effect of dewaxing, 40°C

Name	P_g, GPa
P60	0.37
P60´	0.33
P60D	0.54
P60´D	0.70<

Comparing the interferometric results of the entrapped oils under the Hertzian contact condition, it is noted that as shown in Fig. 9 the fringe patterns of the entrapped hydrocarbon containing fatty acid are characterized by irregular contours and flat bottoms in contrast to those of mineral oils with concentric contours and deep conical bottoms as will be shown later.

As shown in Fig. 11 b), under the Hertzian condition exceeding the freezing pressure the central area of contact is occupied by a dense crowd of thin crystallines which are considered to have little mobility. In contrast to this, the glassy states of the mineral oils in bulk are characterized by the appearance of the atomized granular structure as shown in Fig. 13. This granular structure directly gives evidence of the granular analogy suggested by Gentle and Cameron (5). Consequently, it is reasonable to consider that shear mobility of particles brings about the deep conical entrapment of the mineral oils.

Fig. 15 and 16 show the change in the en-

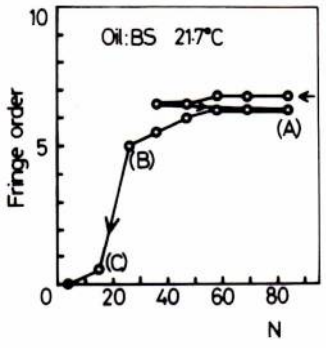

Fig. 15 Change in entrapment in unloading process

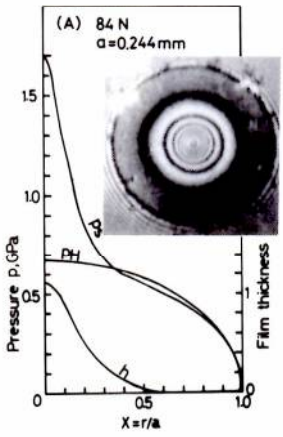

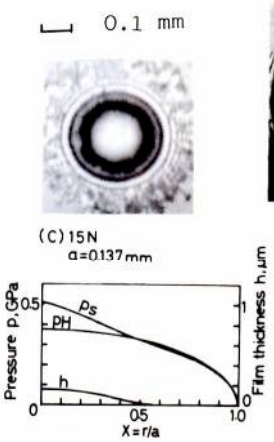

Fig. 16 Pressure (p_S) and deformation (h) at points (A) and (C) in Fig. 15

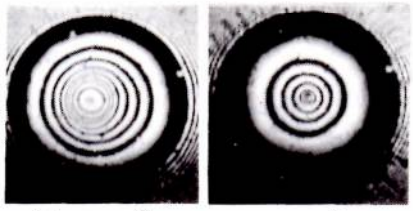

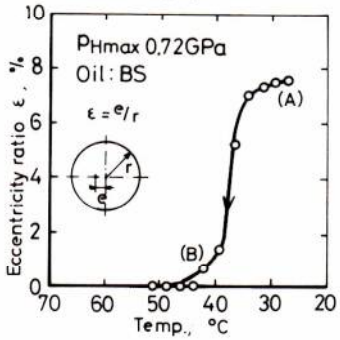

Fig. 17 Change in eccentricity of entrapment

trapped oil BS in the unloading process at room temperature 21.7°C. The initial load 84 N (p_H = 0.67 GPa) was applied by impact from a gap 0.1 mm. In the first unloading process from 84 to 36 N and reversed loading the depth of the entrapment was little changed. Fig. 16 a) depicts the profile of the entrapment indicated by (A) in Fig. 15 and the corresponding pressure distribution numerically estimated (16). The repeated unloading process causes a slow decrease in the entrapment depth up to the point (B), i.e. 26 N, where the sharp profile is still maintained. In the succeeding unloading process to 15 N indicated by (C), however, an abrupt decrease in the entrapped depth occurs. The sharp distribution as in (A) and (B) becomes no more observed.

The glass transition pressure of BS at 21.7°C is estimated as 0.31 GPa. On the other hand, the maximum Hertzian pressures at load 84 (A), 26 (B), and 15 N (C) are 0.67, 0.37, and 0.28 GPa, respectively. Consequently, the glassy state at the maximum Hertzian pressure is considered to disappear during the unloading process from (B) and (C) corresponding to the abrupt decrease in the entrapped depth.

Finally, by observing the change in eccentricity of the contours of the entrapped oil BS in a temperature rise process as in Fig. 17, the feature exhibits the characteristic behaviour corresponding to that in the unloading process in Fig. 15. Thus, the eccentric contours as an evidence of solidification (4) disappears simultaneously with the disappearance of the glassy state.

5. ACKNOWLEDGEMENTS

The present research was supported by a Grant-in-Aid for Scientific Reserch (No. 5935-0011-1984) from Japanese Ministry of Education.

The authors wish to express their thanks to Y. Yamamoto and T. Sakai Kyushu Univ., for their kind support; Y. Nakahara, Saga Univ., for his efforts in preparing the experimental apparatuses; and also to the research members of Idemitsu Kosan Co., especially to N. Takano and T. Kita, who supplied the base oils.

REFERENCES

(1) Smith, F.W., ASLE trans., 3, 18 (1960)
(2) Gentle, C.R. and Paul, G.R., Trans. ASME, JOLT, 98, 258 (1976)
(3) Alsaad, M. et al., Trans. ASME, JOLT, 100, 404 (1978)
(4) Gentle, C.R. et al., Wear, 29, 141 (1974)
(5) Gentle, C.R. et al., Wear, 27, 71 (1974)
(6) Dowson, D. and Jones, D.A., NATURE, 214, May 27, 947 (1967)
(7) Paul, G.R. and Cameron, A., Proc.Roy.Soc. Lond., A, 331, 171 (1972)
(8) Cameron, A. et al., ASLE Trans., 19, 3, 195 (1976)
(9) Hirano, F. et al., Trans. ASME, JOMD, 103, 1, 210 (1981)
(10) Hirano, F., Proc. Shell Industrial Lubricants Tech. Symp., Oct., Tokyo (1980)
(11) Hirano, F., Kuwano, N. and Ohno, N., ASLE Trans., 26, 4, 545 (1983)
(12) Askwith, T.C. et al., Proc.Roy.Soc.Lond., A, 291, 500 (1966)
(13) Hirano, F. and Sakai, T., Proc. 9th Int. Conf. Fluid Sealing, BHRA, 429 (1981)
(14) Nelson, R.R. et al., The Journal of Chemical Physics, 33, 6, 1756 (1960)
(15) Hirano, F., J. JSME, 85, 768, 32 (1982) (in Japanese)
(16) Kuwano, N., Ohno, N. and Muto, T., Rep. Fac. Sci. Engrg. Saga Univ., 12, 103 (1984) (in Japanese)